

Potential impact of earthquakes during the 2020 COVID-19 pandemic

Earthquake Spectra

2021, Vol. 37(1) 73–94

© The Author(s) 2020

Article reuse guidelines:

sagepub.com/journals-permissions

DOI: 10.1177/8755293020950328

journals.sagepub.com/home/eqs**Vitor Silva, M.EERI, and Nicole Paul**

Abstract

The 2020 COVID-19 pandemic caused a human and economic impact of unprecedented magnitude in contemporary history. In an effort to reduce the rate of infection, most governments implemented measures to increase social distancing and to strengthen the capacity of the healthcare system. The occurrence of earthquakes coincident with the pandemic may prevent the effective practice of such measures, and consequently cause an increase in the virus spread. This study analyzes the potential impact that seismic events may have on the infection rate within regions afflicted by both epidemics and earthquakes and explores open software packages that can be employed to simulate the impact of future destructive earthquakes on the spread of an emerging virus. Recent data on the number of confirmed cases at the national or subnational level were combined with a global seismic hazard and risk map to produce a combined index. This index highlights regions where preparedness and contingency plans should be developed to account for the possibility of COVID-19 outbreaks due to the earthquake impact.

Keywords

COVID-19 pandemic, seismic risk, seismic hazard, earthquake scenarios, fatalities

Date received: 29 May 2020; accepted: 7 July 2020

Introduction

The 2020 COVID-19 pandemic has overwhelmed the healthcare system and emergency response capacity of several countries. In an attempt to reduce the number of new infections, several safety measures have been imposed by governmental authorities (the so-called “flattening the curve”). Such measures included the closure of public places, restrictions on gathering size, and the creation of dedicated COVID-19 routes at healthcare facilities. An evaluation of government responses to the COVID-19 at the global scale was performed by Hale et al. (2020). In regions where such measures were endorsed early and

Global Earthquake Model Foundation, Pavia, Italy

Corresponding author:

Vitor Silva, Global Earthquake Model Foundation, Via Ferrata 1, 27100 Pavia, Italy.

Email: vitor.silva@globalquakemodel.org

effectively, there was a reduction in the number of daily confirmed cases (e.g. Gatto et al., 2020; Maier and Brockmann, 2020), thus allowing the healthcare system to better cope with this crisis. Despite the positive impact of such measures, the situation remains precarious in several parts of the world, and the occurrence of a sudden shock (such as an earthquake) in addition to the ongoing strain that COVID-19 presents could bring an otherwise stable emergency response past its coping capacity, causing an increase in the infection rates and associated mortality. For example, after imposing strict measures to reduce the potential spread of the virus, the government of Vanuatu decided to lift social distancing measures to allow the population to escape the devastation caused by the Category 5 Tropical Cyclone Harold. Fortunately, the country had no reported cases¹ prior to the cyclone, and thus the lifting of these measures seemingly had no adverse impact.

A similar situation can be envisaged for regions affected by destructive earthquakes, which arrive without significant advance warning unlike many other natural hazards. The damage caused by seismic events on the residential building stock often requires housing hundreds or thousands of inhabitants in temporary shelters. The 2009 M6.3L'Aquila earthquake damaged more than 35,000 buildings, and left over 45,000 people homeless (Dolce, 2010; Dolce and Di Bucci, 2015). Moreover, the need to treat the injured in the aftermath of an earthquake could cause an excessive influx of people in healthcare facilities and a temporary disregard for rigorous safety measures. In such conditions, social distancing might be impractical, and new clusters of virus spread may arise. It is thus important to account for the possible occurrence of large natural hazards during the pandemic and develop response plans that consider both the constraints due to the pandemic and the additional requirements caused by the natural hazard. As a response to this challenge, some governments have requested their civil protection authorities to create preparedness and contingency plans. However, given the unprecedented situation caused by the COVID-19 pandemic, empirical data regarding the impact that natural hazards might have in the spread of the virus are limited, and consequently such plans might be ill-informed.

In this context, it is convenient to analyze data regarding the possible rise in the daily confirmed cases in regions recently struck by earthquakes and evaluate whether the data provide any evidence of a correlation between seismic events and variations in the infection rates. Such an exercise also allows defining better protocols for data collection, which can inform the development of preparedness plans. Moreover, in the absence of empirical data, it is possible to explore analytical methodologies to simulate different scenarios of earthquake magnitude and COVID-19 infection rates. This process has been followed for decades for the development of post-earthquake response plans (e.g. Italy (DPC, 2018), Turkey (Erdik and Durukal, 2008), Portugal (Mendes-Victor et al., 1994), United States (Detweiler and Wein, 2017), Canada (AIR Worldwide, 2013)), and now it must be expanded to incorporate the potential effects in the spread of an emerging virus.

In this study, data regarding the daily confirmed cases for regions recently struck by damaging earthquakes (e.g. Turkey, Iran, Croatia) were collected at the smallest available spatial and temporal resolution to evaluate the impact on the infection rate. Then, using an open-source software package for seismic hazard and risk analysis, two distinct earthquake scenarios were simulated for Portugal. The results regarding the displaced population (presumed to be more vulnerable to the virus) were used to estimate the potential increase in the number of cases and fatalities, considering different infection rates. Finally, to identify regions in the world where performing such simulations might be particularly important, the most recent data concerning the number of confirmed cases at the national or

subnational level were combined with global seismic hazard and risk maps (Pagani et al., 2020; Silva et al., 2020) to produce a combined index. This index reflects directly areas with significant seismic hazard and/or risk and prevalence of COVID-19 cases.

Impact of past earthquakes during epidemic outbreaks

Epidemic outbreaks following the occurrence of natural hazards are relatively common, particularly in regions with poor sanitary conditions. In 1994, there was a plague outbreak in Western India, three decades after the last case of plague was reported in the region. In the previous year, there was a M6.3 earthquake in Latur that caused almost 10,000 fatalities and widespread damage. Boire et al. (2013) hypothesized that the seismic event disrupted previously stable ecosystems and forced rodent populations to leave their burrows and come in closer contact with human settlements, ultimately leading to the epidemic. A trend between destructive seismic events followed by plague outbreaks has been observed for centuries (Tsiamis et al., 2013). Another example of an epidemic outbreak related to earthquake occurrence was observed in 2010 in Haiti. Eight months after the disastrous M7.0 Port-au-Prince earthquake that caused more than 200,000 fatalities, a cholera outbreak originated from human transmission. Due to the damage caused by the earthquake on the sanitation system and the inadequate healthcare infrastructure already overwhelmed by the injured, this epidemic infected over 650,000 people and caused more than 9000 fatalities.

In addition to the potential changes to ecosystems within the affected areas, natural hazards can cause an accumulation of population in relatively small areas (i.e. crowding), thus creating ideal conditions for the transmission of communicable diseases such as the COVID-19 virus. Watson et al. (2007) summarizes some past examples in which infectious diseases spread among the displaced population. In 1991, the eruption of Mount Pinatubo led to an outbreak of measles that caused more than 18,000 cases among the displaced. Clusters of measles were also reported in Indonesia and Pakistan following the 2004 M9.1 Sumatra and 2005 M7.6 Kashmir earthquakes, respectively. Among the population displaced by these two seismic events, there were also cases and deaths from meningitis and acute respiratory infections (World Health Organization (WHO), 2005, 2006).

For what concerns the impact of earthquakes in ongoing epidemics and other infectious diseases, Suk et al. (2019) present some interesting findings. The authors reviewed 17 studies that reported on suspected or confirmed infectious disease outbreaks following earthquakes and floods in Europe. One of the studies investigated the incidence of infectious diseases following the 2009 M6.3 L'Aquila earthquake (Petrazzi et al., 2013) and concluded that hospital admissions due to infectious diseases rose from 7.41% before the earthquake to 27.18% in the 2 months after the event. The incidence of people with infectious diseases not requiring hospitalization also rose from 12.04% to 27.29%. Another relevant case was reviewed for the city of Lorca in Spain (Pérez-Martín et al., 2017), which was struck by a M5.1 earthquake in 2011. There was an outbreak of chickenpox prior to the earthquake, with 163 cases reported 8 weeks before the event. After the earthquake, 1424 people were evacuated to a temporary shelter, and another 4 cases were detected leading to the declaration of an outbreak. Despite the rapid implementation of a vaccination program, another five cases were identified in the shelter.

At the time of writing of this study, there have been a number of damaging earthquakes in regions with populations infected by COVID-19. The most relevant events include the M6.7 Elazığ (Turkey) on 23 January, the M6.0 near Khoy (Iran) on 23 February, and the

M5.3 Zagreb (Croatia) on 22 March. A key aspect for the evaluation of the impact of these seismic events on the COVID-19 pandemic is undoubtedly how aggressively each country is testing their population, and how the data are being released. Turkey reported its first case in Istanbul on 11 March, almost 50 days after the M6.7 Elazığ earthquake, thus no correlation can be observed. In Iran, the first case was reported in the city of Qom on 19 February, a few days before the seismic event, which could mean that some cases already existed in the west of the country where the earthquake struck. However, the sub-national data indicate no COVID-19 cases prior to the seismic event in the province of West Azerbaijan (where the epicenter of the event is located), and less than 40 cases were reported in the 14 days after the event. It is thus reasonable to assume that even if the impact caused by the seismic event could increase the transmissibility of the virus, there were insufficient cases to trigger an outbreak.

In Croatia, the M5.3 Zagreb earthquake occurred 1 month after the first reported COVID-19 case in the capital, and thus it is relevant to carefully analyze the damage caused in the city and the evolution of the number of cases. This event damaged about 250 houses and 59 people required temporary shelters, while 1 person died and at least 27 suffered injuries (Quigley et al., 2020). Before the earthquake, 87 COVID-19 cases had been reported in Zagreb, and 206 in the entire country according to the Croatian Institute of Public Health.² In the following 2 weeks, 337 more cases were reported in Zagreb (the region most affected by the earthquake). The daily new cases for Croatia at the sub-national level are presented in Figure 1.

The evolution of the virus spread in Croatia shows a significant increase in the daily cases in the 2 weeks after the seismic event. Although it is plausible to presume that the potential disruption in the safety measures due to the earthquake contributed to this rise, there are other factors that could have played a role. For example, on 19 March (4 days before the earthquake), the Croatian government imposed strict measures to reduce the spread of the virus. Clearly such measures would not have been able to demonstrably flatten the infection curve until after 2 weeks, which could explain the steep increase in this period followed by a more constant number of daily new cases. Moreover, across Europe, the number of tests per habitant increased significantly once the government declared a national lockdown. This increase in the number of cases could also be explained by more aggressive testing within the population during this time frame. Finally, shortly after the

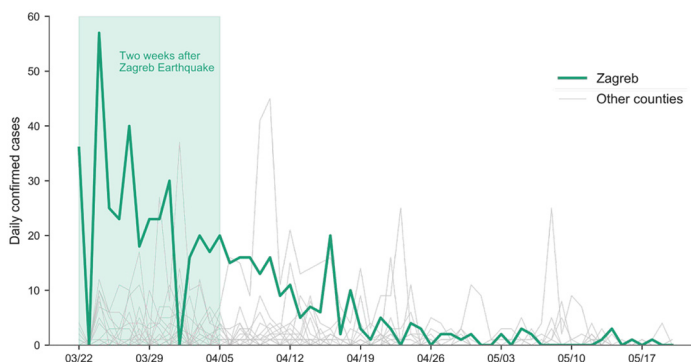


Figure 1. Daily confirmed cases in Croatia by county according to the Croatian Institute of Public Health.

earthquake, the Croatian government issued directives to implement new safety measures (Quigley et al., 2020). The M5.3 Zagreb earthquake is perhaps a positive example of how rapid and effective action can prevent the increase in the transmissibility of the virus, as opposed to a scenario in which a natural hazard led to new clusters of disease, as previously reported for India, Indonesia, and Pakistan in outbreaks prior to COVID-19. Other events have also been considered for this evaluation, including the M5.7 Magna earthquake in Utah (18 March) and the earthquake swarm that affected the southern region of Puerto Rico in the beginning of 2020. However, for the same reasons described above for Iran, no significant increase in the number of COVID-19 cases was found.

For more information regarding the impact of other meteorological and geophysical hazards during the 2020 COVID-19 pandemic, readers are referred to Quigley et al. (2020).

Simulation of potential COVID-19 spread due to seismic events

The simulation of earthquake and infection scenarios can provide relevant information to support the development of preparedness and contingency plans. Such simulations have been used for decades for the development of post-earthquake response plans (e.g. Erdik and Durukal, 2008; Mendes-Victor et al., 1994), evaluation of temporary housing needs (e.g. Anhorn and Khazai, 2014), and improvement of urban planning (e.g. Sengezer and Koç, 2005). The same knowledge can be expanded to the assessment of the potential effects that an earthquake can cause in the infection rates, and consequently in the number of new cases and fatalities. This process is demonstrated herein using two earthquake scenarios for Portugal with distinct geographical and tectonic characteristics. Then, using the displaced population estimates, several epidemiological simulations were performed considering different assumptions for the infection rates.

Description of the earthquake scenarios

Portugal has been the target of several past studies regarding the impact of specific earthquake scenarios (Mendes-Victor et al., 1994; Oliveira, 2004; Silva et al., 2015), which were then used to support governmental authorities in the development of response plans. Due to the concentration of population and moderate-to-high seismic hazard in the southwest of the country, two earthquake scenarios are usually considered (Carvalho et al., 2008; Oliveira, 2008): a moderate magnitude event onshore near the Metropolitan Area of Lisbon, and a strong magnitude event offshore (located in a region presumed to have generated the 1755 Great Lisbon Earthquake, e.g. Sousa and Campos-Costa, 2009). The characteristics of these two events are summarized in Table 1.

The distribution of the ground shaking generated by these events in the country was computed using the OpenQuake-engine (Pagani et al., 2014). The ground motion prediction equations (GMPEs) from Atkinson and Boore (2006) and Akkar and Bommer (2010) were used in this process for the onshore and offshore events, respectively, as they allow

Table 1. Characteristics of the selected earthquake ruptures

Rupture	Magnitude (M_w)	Strike	Dip	Rake
Onshore	5.7	220°	55°	0°
Offshore	8.7	35°	40°	90°

the consideration of site effects and compared well with instrumental and intensity observations for the country (Vilanova et al., 2012). The consideration of site effects was performed using the site model described in Silva et al. (2014b).

Vulnerability, exposure, and COVID-19 data

For the estimation of the impact in terms of fatalities and population displaced by the aforementioned earthquake scenarios, the fragility functions proposed by Martins and Silva (2020) and the exposure model developed within the H2020 European SERA project (Crowley et al., 2020) were employed.

The fragility functions were developed using an analytical approach. Each building class was represented by a single-degree-of-freedom (SDoF) oscillator characterized by the capacity spectrum relation (spectral displacement— S_d vs spectral acceleration— S_a). Then, each oscillator was subjected to nonlinear dynamic analysis using a database of 3500 ground motion records that consider a range of magnitudes, distances, and tectonic environments (including stable and active shallow regions relevant to Portugal). After the nonlinear time history analysis, the response (in terms of spectral displacement) was classified into four damage states: slight, moderate, extensive, and complete damage. For each damage state, a fragility curve is fitted using the cloud analysis methodology proposed by Jalayer et al. (2015). Additional information regarding the derivation process can be found in Martins and Silva (2020), while the procedure used to employ these functions in the estimation of fatalities and population displaced is described in the following section.

The exposure model was developed based on the latest national housing census, and it includes information about the main construction material, lateral load resisting system, number of stories, and date of construction (used herein as a proxy for the seismic design level). The exposure model was defined at the third administrative level (i.e. parishes), and the number of occupants per building was computed based on the average number of dwellings per building class and the average number of occupants per dwelling. Additional information concerning the exposure derivation procedure can be found in Crowley et al. (2020). In addition to the information regarding the building stock, the estimation of the increase in the COVID-19 cases and related fatalities required detailed data regarding the number of confirmed cases, transmissibility factors, and mortality rates for Portugal. In this study, the data released by the National General Health Directorate³ and compiled in a public GitHub⁴ repository by the Data Science for Social Good⁵ group were used. Figure 2 presents the number of buildings (left) and number of confirmed COVID-19 cases (right—as of 22 May 2020) for mainland Portugal. Both indicators are presented at the second administrative level (e.g. county) for visual clarity. The boundaries of the five administrative regions (i.e. north, center, Lisbon and the Tagus Valley, Alentejo, and Algarve) that have been used to communicate the spread of the COVID-19 virus in Portugal are also presented in this figure and will be used to illustrate the increase in the number of cases at the subnational level due to the earthquake impact.

Estimation of fatalities and population displaced

The estimation of human impact caused by the two scenarios was performed using the scenario damage calculator of the OpenQuake-engine (Silva et al., 2014a). In this process, the previously described ground motion fields and the fragility and exposure models (described in section “Vulnerability, exposure, and COVID-19 data”) are combined to estimate the

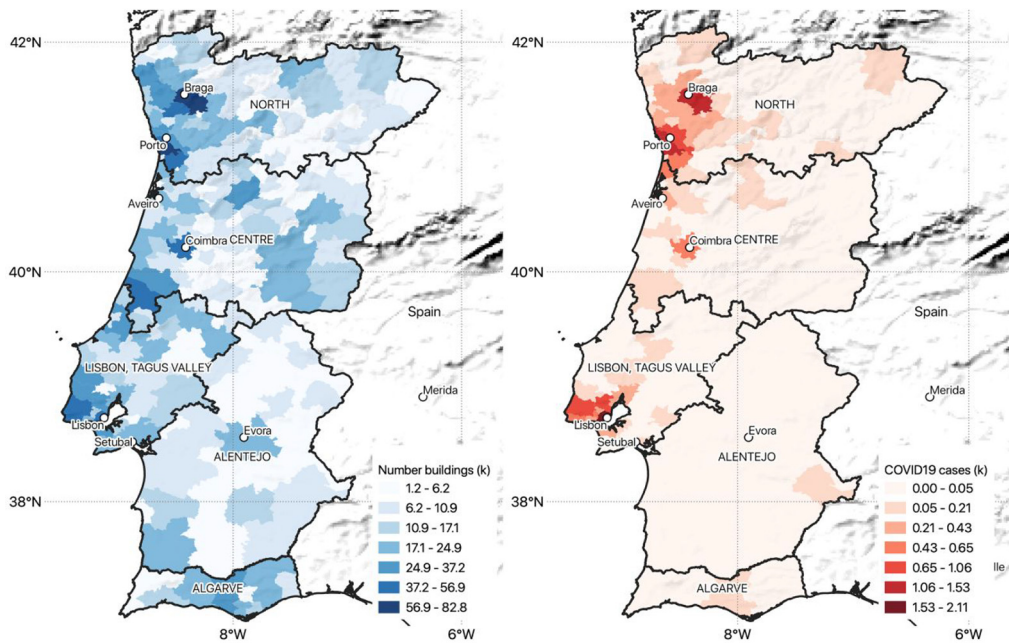


Figure 2. Number of residential buildings (left) and confirmed COVID-19 cases (right—as of 22 May 2020) at the county level in Portugal.

number of buildings in each damage state. This damage distribution can then be used to estimate the number of injured and fatalities using a consequence model (e.g. Coburn and Spence, 2002; Spence, 2007). For the purposes of this study, we have focused only on fatalities and the population left homeless. However, we recognize that the number of injured is also a relevant indicator to assess the impact of earthquakes during a pandemic. For the former metric, it is necessary to estimate the portion of structural collapses from the amount of buildings assigned to complete damage. For this step, we used the probabilities of collapse given complete damage proposed by FEMA P58 (2012), which take into consideration the type of construction and seismic design level. The number of fatalities is then estimated by considering the number of occupants in collapsed buildings, using a fatality rate. We adopted the rates proposed by Spence (2007), which accounts for the type of construction and number of stories.

To estimate the population displaced, all buildings that had at least moderate damage were presumed unable to be immediately occupied, and thus their occupants would have to be moved to temporary housing or shelters. The 2009 M6.3L'Aquila earthquake in Italy left about 45,000 people homeless. Half of the homeless were temporarily rehoused in hotels on the Adriatic Sea coast of Abruzzo and the other half was accommodated in 171 shelters (Dolce, 2010). Regardless of the solution adopted by the displaced population, it is evident that the exposure to the virus can increase. Figure 3 presents the mean number of people left homeless at the county level for the two earthquake scenarios. For what concerns human losses, the onshore and offshore scenarios caused a mean death toll of 292 and 1729, respectively. We note that due to the propagation of the epistemic and aleatory uncertainty in the GMPEs and fragility functions, the damage distribution is characterized by a probability distribution. The variability in the number of displaced population will be

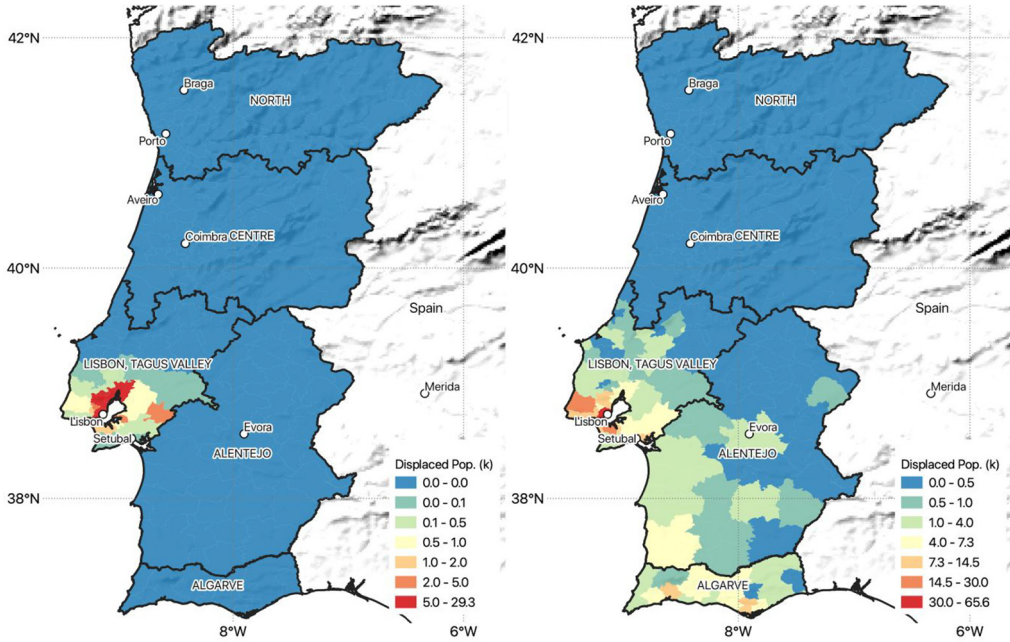


Figure 3. Displaced population at the country level for the M5.7 onshore (left) and M8.7 offshore (right) earthquake scenarios.

further propagated into the computation of the number of additional COVID-19 cases, as further described in the following sections.

Definition of the COVID-19 spread cases

The pathogen transmissibility of epidemics is commonly characterized by the effective reproduction number (R_t), which represents the average number of new infections caused by a single infected individual at time t in the partially susceptible population (e.g. Anderson and May, 1991). There are various methods to estimate the R_t factor (e.g. Amundsen et al. 2004; Cintron-Arias et al., 2009; Riley et al., 2003), with varying levels of complexity and reliability. In this study, we measured the R_t factor for Portugal and sub-national regions using a well-established and simple method that assumes that the daily incidence (i.e. number of new cases— I_t) can be approximated by a Poisson process, as described by the following equation (e.g. Fraser, 2007):

$$I_t \sim \text{Pois} \left(R_t \sum_{s=0}^t I_{t-s} w_s \right) \quad (1)$$

where w_s represents the transmissibility profile of each infected case, and it depends only on the time since infection. Although w_s will depend on individual biological factors such as pathogen shedding or symptoms severity (Cori et al., 2013), it can be reasonably approximated to the serial interval (i.e. the time between the onset of symptoms in a

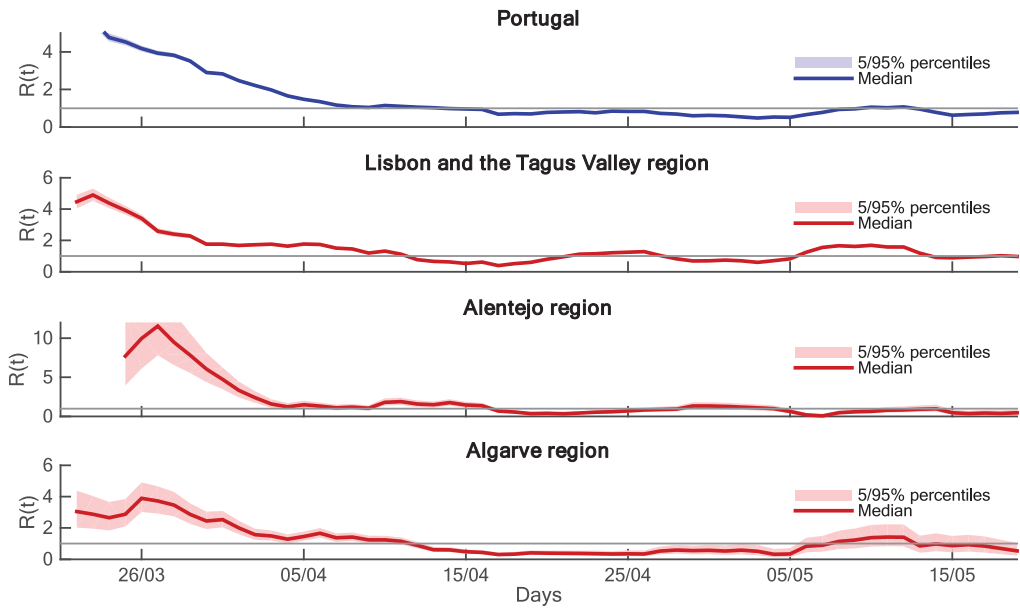


Figure 4. Effective reproduction number (R_t) for Portugal and subnational regions of Lisbon and the Tagus Valley, Alentejo, and Algarve.

primary case and the onset of symptoms of secondary cases) assuming a Gamma distribution. We assumed a mean of 6.5 days and a standard deviation of 3.8 days based on the revision of transmissibility cases in Wuhan (China) performed by Ferguson et al. (2020). Under this assumption, an individual is most infectious at the 4th day of infection, and after the 10th day, the transmissibility probability decreases to values below 5%. The number of cases for each day was extracted from the previously mentioned public GitHub⁶ repository. Following this method, the median R_t factor (and associated percentiles) for Portugal and three subnational regions was estimated, as presented in Figure 4. We present only the R_t factor for the subnational regions (Lisbon and Tagus Valley, Alentejo, and Algarve) which are expected to be affected by the earthquake scenarios described previously. The General Health Directorate indicated that the peak of the infection in Portugal occurred sometime between 20 and 25 March.

Equation 1 can also be used to forecast the evolution of the number of incidences in a given region using a Markov Chain Monte Carlo (MCMC) sampling method (e.g. Nouvellet et al., 2018). In this process, the R_t factor is sampled from the joint posterior distribution, and at each MCMC iteration, the new cases are incorporated in the sampling process. This procedure allows propagating the uncertainty in R_t , as well as to incorporate changes in the transmissibility due to the occurrence of external events (such as earthquakes) or the introduction of measures to reduce the infection ratio. As described in the previous section, current data regarding the occurrence of natural hazards during the 2020 COVID-19 pandemic are scarce and statistically insufficient to properly evaluate how natural hazards might aggravate the transmissibility. Nonetheless, it is possible to explore the limited data reflecting different stages of the pandemic to define plausible scenarios of

infection for the displaced population. We have defined two plausible cases of transmissibility as described below:

- *Case A.* This case represents an optimistic scenario in which the R_t factor slightly increases after the seismic event, and then decreases at a rate similar to the one observed for the associated region prior to the seismic event. We assumed a value for R_t equal to the one registered 2 weeks after the declaration of the emergency state in Portugal (i.e. $R_t \sim 2.5$). The 2 weeks after this declaration represents a period where despite the strict policy measures to curb the infection rate, some equipment was still missing and the population was still adapting to the new directives. This scenario aims to reflect a situation in which some level of preparedness from the emergency authorities exists, but the disruption caused by the seismic event did not allow for the population to fully follow all of the directives adequately.
- *Case B.* This case represents a more pessimistic scenario where the R_t would increase sharply after the seismic event. For this scenario, we assumed an increase of the R_t factor to the value registered in Portugal during the peak of the infection (i.e. $R_t \sim 4.1$, 20–25 March, as indicated by the General Health Directorate). This case represents a scenario in which the emergency authorities and the population are ill-prepared, and the safety measures either do not exist or are unable to be properly followed.

It is important to mention that these scenarios of infection were only applied to the displaced population (i.e. people whose dwellings had at least moderate damage). This hypothesis is supported by the findings from the previous section, which presented several past cases of disease outbreaks among the population displaced. The propagation of the virus among the remaining population was assumed to follow the trend registered in the previous week. The number of new incidences is then expressed by the following equation:

$$I_t \sim \text{Pois} \left(R_t \sum_{s=0}^t I_{t-s} w_s \times (1 - P_{\text{disp}}) \right) + \text{Pois} \left(R_t^{A/B} \sum_{s=0}^t I_{t-s} w_s \times P_{\text{disp}} \right) \quad (2)$$

where P_{disp} is the probability that a given individual will be displaced, as estimated by the OpenQuake-engine, and $R_t^{A/B}$ represents the effective reproduction number assumed for Case A or B. We recognize that for large destructive events, the transmissibility rate even among the population that was not displaced might increase, though this effect was not considered in these analyses. The impact of these assumptions in the results is further discussed in the concluding remarks.

The prediction of the number of additional cases was performed for 4 weeks following the seismic event. A prediction period longer than this was deemed unrealistic due to the volatility of the virus spread. To compare the impact of these two scenarios against the case in which no earthquake occurs, we have also estimated the expected increase in the number of cases and fatalities using the mean R_t factor registered in the previous week in the three subnational regions affected by the earthquake scenarios.

Forecasting COVID-19 cases due to the earthquake impact

For the estimation of the new cases and fatalities due to COVID-19, the main hypothesis is that the population left homeless will be particularly vulnerable to infection due to the

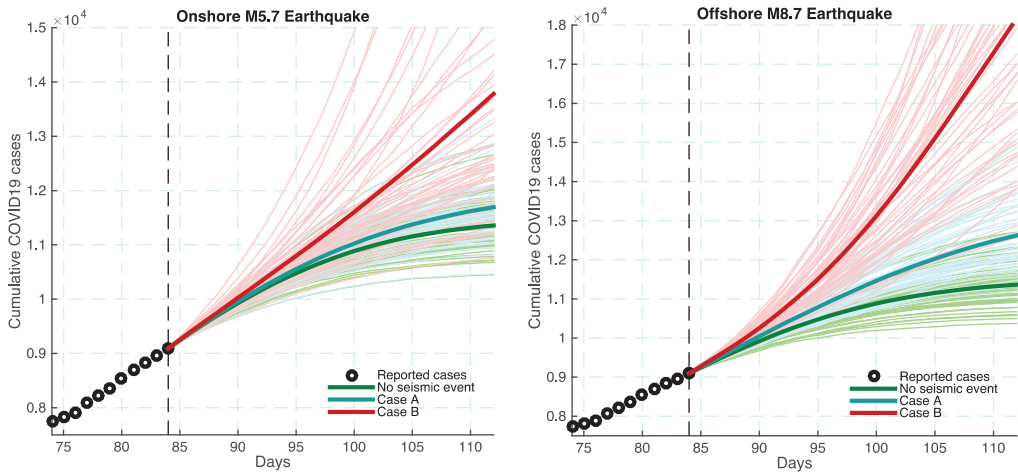


Figure 5. Forecasting of the (aggregated) number of cumulative COVID-19 cases for the three regions (Lisbon and the Tagus Valley, Alentejo, and Algarve) considering the displaced population from the M5.7 onshore (left) and M8.7 offshore (right) earthquake scenarios. The darker line represents the mean results, while the lighter lines represent individual simulations.

inability to comply with the safety regulations. Some of the factors could include the inability to maintain proper social distancing during temporary housing, lack of protective equipment caused by disruption of supply chains, or the need to use healthcare facilities due to injuries, which might be overwhelmed and unable to maintain all safety measures. We note once again that during the simulation of the new cases, both the uncertainty in the estimation of the displaced population and the R_t factor are propagated, leading to hundreds of simulations of new COVID-19 cases. Figure 5 presents the simulated evolution of the aggregated number of cases (i.e. sum of the cases for the three regions) for the 4 weeks after the seismic event, considering the onshore (left) and offshore (right) scenarios, and the three transmissibility assumptions (i.e. no seismic event, Case A and Case B). The darker line represents the mean cumulative COVID-19 cases for each transmissibility case, while the lighter lines represent individual simulations, which can also be used to estimate error bars around the mean results or specific percentiles.

The results indicate, as expected, striking differences between Case A and Case B, highlighting the importance of rapidly imposing measures to reduce the transmissibility of the virus. Given the different geographical extents of the two earthquake scenarios, it is also important to evaluate the potential impact of these events at the subnational level. Figure 6 illustrates the increase (as a percentage) in the number of cases per region, following the previously presented administrative organization of the country.

Regarding the additional fatalities caused by the COVID-19 virus, the mortality rate (M_r) in Portugal (according to the data released by the General Health Directorate) has been stable at 4.3%. However, this rate reflects a situation in which the healthcare system is not overwhelmed with the injured by the earthquake and additional population infected. Other European countries heavily affected by the COVID-19 pandemic registered mortality rates⁷ of 11.5% (Spain), 13.9% (United Kingdom), 14.3% (Italy), and 19.6% (France). In this study, to account for both situations (i.e. stable and overwhelmed healthcare system), the mean number of fatalities due to the increase in the number of COVID-19 cases

Table 2. Mean number of additional fatalities due to the increase in the number of COVID-19 cases caused by the earthquake impact

Transmissibility case	M5.7 Onshore earthquake			M8.7 Offshore earthquake		
	Due to the additional COVID-19 cases		Due to structural collapses	Due to the additional COVID-19 cases		Due to structural collapses
	$M_r = 4.3\%$	$M_r = 11.5\%$	292	$M_r = 4.3\%$	$M_r = 11.5\%$	1729
Case A	0.6	1.6		51.6	138.0	
Case B	2.4	6.4		256.7	686.5	

were computed considering both the current mortality rate for Portugal and the one reported for Spain, as described in Table 2. We recognize that such rates are heavily affected by the number of reported cases (and hence the large discrepancies among these countries) and may not represent a realistic mortality rate. Nonetheless, the projections performed in this study were also based on the number of reported cases and not actual number of infected. For the sake of completeness, the mean number of fatalities caused by the collapse of residential buildings is also presented in Table 2.

The impact of the various assumptions adopted in these analyses and the differences in the results between the earthquake scenarios and transmissibility cases are further discussed in the following section.

Discussion of results

The results from Figure 6 illustrate important differences in the increase of COVID-19 cases across the three regions. For the onshore event which affects mostly the population in Lisbon and the Tagus Valley (i.e. 1.9%), when effective measures to limit the transmissibility of the virus are assumed (i.e. Case A), the impact is limited (i.e. less than 1% increase in the number of cases). This outcome seems to be in agreement with the observations from the 2011 M5.1 Lorca (Spain) and 2020 M5.3 Zagreb (Croatia) earthquakes, where the seismic damage was also relatively localized, and the government acted quickly to counter the infection rate. On the other hand, for the case where the transmissibility rate increased considerably (i.e. Case B), even an event with limited impact was able to cause a significant increase in the number of cases (i.e. 10.3%). For the offshore event, which caused widespread damage and more than 350,000 people were left homeless, the increase in the COVID-19 cases is substantial even in the more optimistic transmissibility case. Such an outcome indicates that stricter and more effective measures would have to be rapidly implemented in order to counter the spread of the infection. It is also interesting to note that despite the fact that a greater fraction of the population was affected in Algarve (i.e. 13.3%) than in the Lisbon and Tagus Valley region (i.e. 8.3%), the increase in the number of COVID-19 cases is greater in the latter region. This outcome is due to the discrepancy in the number of reported cases between the two regions. At the time of writing of this study, the southern region of Algarve had less than 400 confirmed cases, while Lisbon reported more than 9000.

It is also relevant to discuss some of the assumptions that had to be adopted in these analyses, and how they might be influencing the results. It was assumed that the

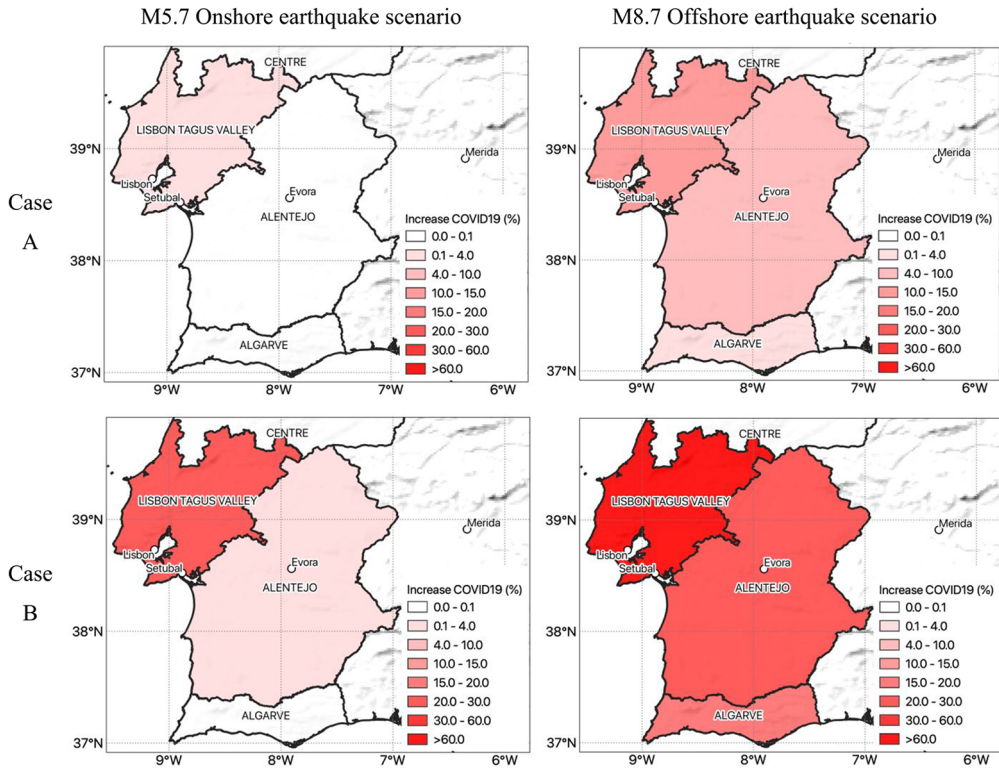


Figure 6. Estimated increase in the number of cumulative COVID-19 cases (as a percentage) for the three regions (Lisbon and the Tagus Valley, Alentejo, and Algarve) considering the M5.7 onshore (left) and M8.7 offshore (right) earthquake scenarios, and Case A (top) and Case B (bottom) of virus transmissibility.

percentage of cases in the group of people affected and not affected by the seismic event is the same. These fractions can vary spatially, depending on the location of the clusters of infection (see Figure 2) and distribution of the damage. Moreover, the higher transmissibility rates are only being applied to the population that was left homeless, and consequently potentially unable to maintain all safety measures. However, this assumption might not hold for the fraction of the population that will find safer housing solutions, such as a secondary home that can allow the occupants to maintain social distancing. On the other hand, these analyses do not account for the additional population that will move to the affected areas to provide assistance to the injured and displaced, assess structural damage, and plan the reconstruction process. These analyses also did not account for the possibility of strong aftershocks that might displace additional population. Moreover, healthcare staff, even in areas far from the epicenter, might be affected due to the need to treat the injured that might be infected. These analyses assumed that the displaced population will remain in the respective region. While this was the tendency in past earthquakes (e.g. 2009 L'Aquila earthquake—Dolce, 2010), alternative housing solutions might be found outside of the respective region. Finally, it is also important to mention that in the aftermath of the seismic event, the population whose housing was undamaged might be also unable to return to their homes for several days or weeks due to the need to perform

safety assessment, or simply due to the disruption of basic utilities (e.g. water supply, power grid). In these conditions, the total population left more vulnerable to the virus will be greater than the one considered in this study. In summary, while there are assumptions in this study that might be rather pessimistic (i.e. all population displaced will be affected by a higher virus transmissibility), there are also several factors that could have increased the rate of infections both inside and outside of the affected regions. The incorporation of these aspects without additional data, in the authors' opinion, would be too speculative. In fact, the consideration of the variability in the displaced population and in the effective reproduction number alone is sufficient to introduce a large variability in the expected number of new COVID-19 cases, as illustrated in Figure 5.

Identifying regions of high seismic and COVID-19 combined risk

On 13 May, the WHO declared that the COVID-19 virus might become endemic, and in practice never be completely wiped out. It is therefore likely that some parts of the world will be struck by damaging earthquakes while the number of active COVID-19 cases is still high. It is important to identify regions of particular concern and develop or improve emergency response plans to account for the requirements and constraints imposed by the virus. In this study, we propose a qualitative classification of the globe, considering the number of COVID-19 cases per 1 million habitants and a recent evaluation of the seismic hazard and risk.

For the classification of the world based on the virus prevalence and the regional seismic hazard and risk, we used a bivariate scaling system. This qualitative approach is often used to depict pairs of variables whose mathematical combination might not be straightforward or possible, such as social vulnerability and natural hazards (e.g. Emrich and Cutter, 2011). In this process, two thresholds are defined to classify each variable into low, moderate, and high. Then, a color matrix comprising all of the combinations between the two variables is created. In this study, we combined the number of COVID-19 cases per 1 million habitants with two other variables: (1) seismic hazard in terms of the peak ground acceleration (PGA) for the 475 year return period and (2) average annual losses normalized by the local construction cost. The data concerning the number of COVID-19 cases per 1 million habitants at the national scale were extracted from the Johns Hopkins University public GitHub repository,⁸ which in turn collects data from the various national statistical offices or ministries of health. For large countries with high numbers of reported COVID-19 cases and moderate to high seismic hazard or risk (e.g. Silva et al., 2020), additional data were collected at the first administrative level, thus allowing a more detailed view of the spatial distribution of the virus threat. These include Australia, Brazil, Canada, Chile, China, India, Italy, Iran, Japan, Mexico, Peru, Russia, Spain, and the United States. For other countries where such a step would also be desirable (e.g. Ecuador, Pakistan, and Turkey), the data did not seem to be promptly available. Figure 7 presents the number of COVID-19 cases per 1 million habitants at the national (in shades of red) or subnational (in shades of blue) level (as of 2 July 2020). As previously mentioned, these values are heavily affected by how aggressively each country has been testing their population. Therefore, the results for some countries might seem less concerning due to the fact that an important portion of the infected are not accounted for. The cumulative number of tests per country per 1 million habitants can be found at Worldmeter.⁹

The seismic hazard estimates were extracted from the global seismic hazard map produced by Pagani et al. (2020). This map was generated using a mosaic of regional (e.g.

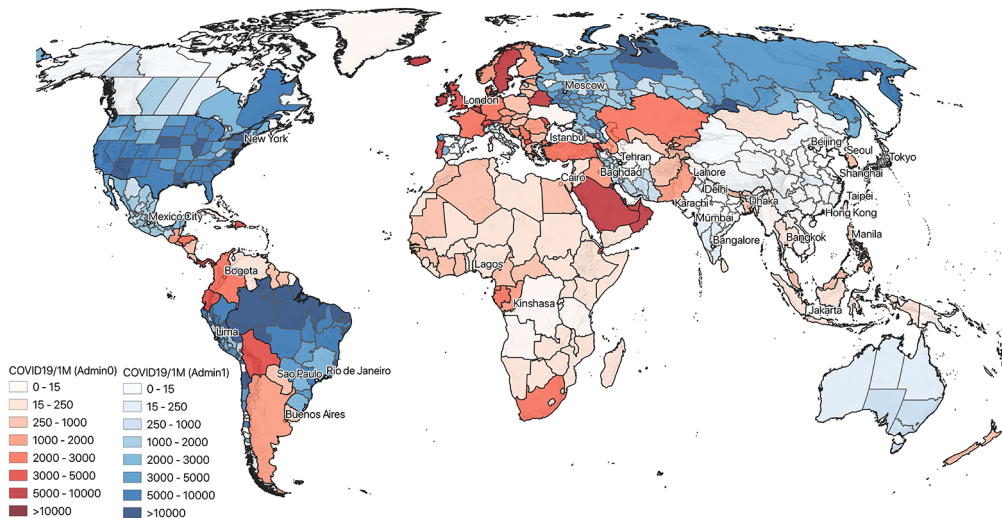


Figure 7. Number of confirmed COVID-19 cases per 1 million habitants at the national (in shades of red) or subnational (in shades of blue) level (as of 2 July 2020).

South and Central America, Central Asia, sub-Saharan Africa, Europe) and national (e.g. Canada, United States, Indonesia, Australia, New Zealand, Philippines, South Africa) seismic hazard models. The hazard is expressed in terms of the PGA (as a fraction of g) for a probability of exceedance of 10% in 50 years (equivalent to a 475 year return period) on rock (average shear-velocity down to 30 m - $V_{s30} = 760$ m/s). A detailed description of how the global seismic hazard model was developed can be found in Pagni et al. (2020).

Concerning the seismic risk estimates (which accounts for the seismic hazard, exposure, and vulnerability of the building stock), the average annual losses were extracted from the global seismic risk map produced by Silva et al. (2020). This map was generated using the previously described global seismic hazard model; a global exposure model covering the residential, commercial, and industrial building stock; and a set of global vulnerability functions (Martins and Silva, 2020). In order to allow a comparison between different countries, the average annual losses were normalized by the average local construction cost per square meter. This normalization allows comparing the risk between countries with significantly different construction costs. In practice, it reflects the average annual area lost due to earthquakes, which will naturally have a strong correlation with displaced population. Additional details regarding the global seismic risk model can be found in Silva et al. (2020). Both global maps follow an evenly spaced hexagonal grid with a 0.30×0.34 decimal degrees resolution, which is approximately equal to 1000 km^2 at the equator.

The thresholds defined to classify each variable into low, moderate, and high are presented in Table 3. Each threshold was defined to simply allow a clear distinction between the current characteristics of each region and do not have a particular physical meaning.

The combination between the number of COVID-19 cases per 1 million habitants and seismic hazard is presented in Figure 8. This map explicitly highlights regions in the world with substantial COVID-19 cases per 1 million habitants along with a simultaneous higher likelihood of experiencing strong ground shaking. Some of these regions include Chile,

Table 3. Thresholds defined to classify each variable (number of COVID-19 cases per 1 million habitants, seismic hazard, and seismic risk) into three categories: low, moderate, and high

			Number of COVID-19 cases per 1 million habitants		
	Seismic hazard	Seismic risk	Low $N < 500$	Moderate $500 < N < 5000$	High $N > 5000$
High	$PGA > 0.2g$	$AAL > 5000$			
Moderate	$0.1g < PGA < 0.2g$	$1000 < AAL < 5000$			
Low	$PGA < 0.1g$	$AAL < 1000$			

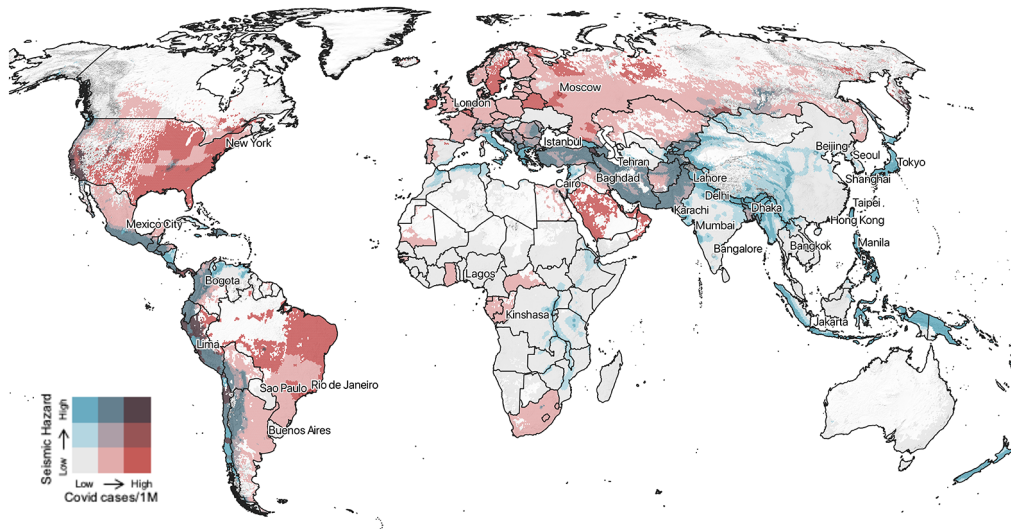


Figure 8. Bivariate maps depicting the combination of seismic hazard and the number of confirmed COVID-19 cases per 1 million habitants (as of 2 July 2020).

Peru, Ecuador, Turkey, Iran, Italy, the Dominican Republic, Panama, and the west of the United States.

The use of seismic hazard to characterize the threat posed by earthquakes has the advantage of being easier to understand by a less technical audience (due to the frequent use of hazard maps for building regulations) and of having a lower number of sources of uncertainty (as opposed to seismic risk which is also affected by the uncertainty in the exposure and vulnerability). However, it does not account for the expected physical impact (i.e. damage and losses), which is fundamental for the purposes of this study. Figure 9 presents the combination between the number of COVID-19 cases per 1 million habitants and seismic risk. In comparison with the previous global map, this exercise allows identifying urban centers with both high prevalence of COVID-19 cases and earthquake risk. Some of these large urban centers include Istanbul and western Turkish cities, the Po Valley in Italy, the Great Metropolitan Area of Lisbon, San Francisco Bay Area, Greater Los Angeles, US cities (e.g. Saint Louis, Memphis) near the New Madrid seismic zone, Tehran and other Iranian cities along the southern border, the Great Metropolitan Area

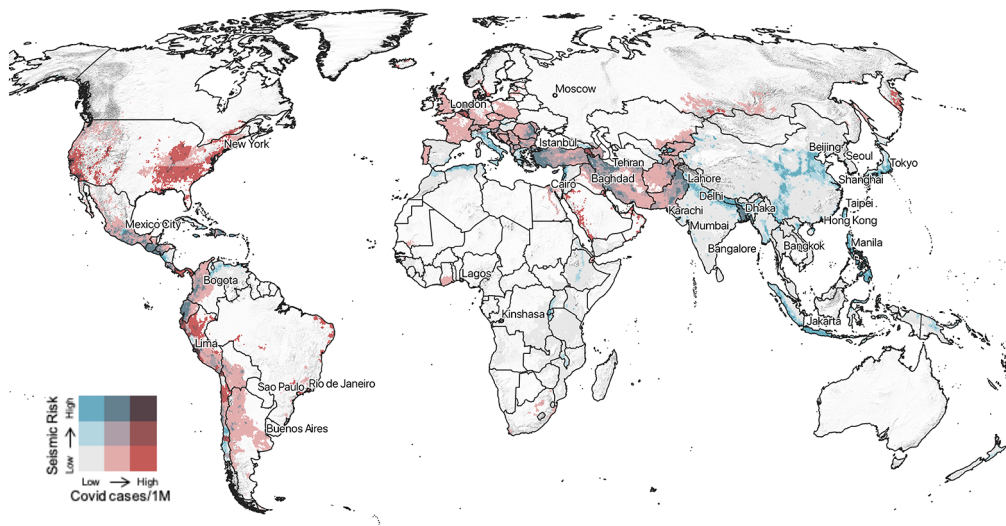


Figure 9. Bivariate maps depicting the combination of seismic risk and the number of confirmed COVID-19 cases per 1 million habitants (as of 2 July 2020).

of Santiago, Lima and Callao, Santo Domingo and Santiago de los Caballeros, Panama City, the metropolitan areas of Quito and Guayaquil, and the Greater Tokyo Area. These are regions where additional (and more detailed) analyses such as the ones presented in the previous section for Portugal might be useful to inform the development of preparedness and contingency plans. It is interesting to note that both the simulations presented previously and the results from this section highlight the Metropolitan Area of Lisbon as a region of particular concern regarding the potential increase in the number of COVID-19 cases due to earthquakes.

Conclusion

Both recent and ancient history have documented the rise and spread of infectious diseases due to destructive earthquakes. The global prevalence of the COVID-19 virus brings unprecedented challenges to disaster risk management, and in particular, to the adoption or development of response and preparedness plans for coincident natural hazard events. National civil protection authorities and international organizations with the remit to prepare and respond to catastrophic events will have to go beyond the consideration of the direct impact of natural hazards and account for the additional requirements and constraints imposed by the COVID-19 pandemic.

This study presented a framework for the analytical estimation of the amount of population left homeless due to an earthquake scenario, and simulation of the expected increase in the number of COVID-19 cases due to the plausible possibility that not all of the safety measures will be respected. Different cases of transmissibility (i.e. optimistic and pessimistic scenarios) were considered, leveraging on data regarding the effective reproduction number (R_t) and deceleration rates observed in Portugal since February 2020. Such analyses elucidate the factors driving the evolution of the number of daily cases in a particular region, and the potential additional strain upon the healthcare system if an event of

similar characteristics were to happen. For the particular case of Portugal, it was observed that if the effects of an event with a localized impact are managed rapidly and efficiently (i.e. leading to low transmissibility rates), the increase in the number of additional COVID-19 cases would be negligible. For large events in which a considerable amount of the population is likely to be affected, a rise in the virus spread might be inevitable, even assuming an optimistic scenario of emergency response. Given the results presented herein, governmental agencies with the remit to rapidly estimate and communicate the direct impact of earthquakes could include information in such reports concerning the number of cases and highest observed reproduction number in the region.

The investigation of disease outbreaks following destructive earthquakes and the analytical results from the earthquake scenarios clearly demonstrate the need to better identify regions of particular concern and to develop adequate response and preparedness plans. In this context, this study explored data concerning the number of COVID-19 cases at national or subnational scale and recent models characterizing earthquake hazard and risk at the global scale. Seismic hazard was represented by the PGA on rock for the 475 year return period while seismic risk was expressed in terms of average annual losses. Both metrics are commonly used within the respective communities, but it is recognized that other indicators could have been used, such as probable maximum losses (PMLs) for risk. PMLs could potentially change the pattern in the results presented herein, in particular for regions whose seismic risk is driven by events with a long return period (e.g. South of Portugal, Central United States). The combination of these variables allowed highlighting regions and urban centers in the world where the development of mitigation actions is crucial. At the time of writing of this study, some of these urban centers (e.g. cities in South America along the Pacific coast and in the Middle East) were already overwhelmed by the human and economic impact caused by the virus. The occurrence of a damaging seismic event without a proper response plan could lead to the collapse of the healthcare system and a steep increase in the mortality toll.

The manner in which the seismic hazard and risk metrics were combined with the COVID-19 indicator conflates two timescales. The former metrics are time-independent, while the latter simply represents the number of confirmed cases at a certain point in time, thus neglecting whether the number of cases is increasing or decreasing. The identification of the regions with high combined earthquake and COVID-19 risk could benefit from an equally valid time-independent COVID-19 indicator, reflecting both the likelihood of a pandemic outbreak and the capacity of a given region to cope with the consequences of an emergent virus. Such indicator could incorporate data regarding population density, demographic characteristics (e.g. age, gender), predisposition to follow safety measures, and capacity of the healthcare infrastructure. The development of such index was out of the scope of this study.

Although not investigated herein, there is another adverse effect caused by the combination of natural hazards during pandemics that might be critical. In countries that often rely on international aid to cope with catastrophes, travel restrictions and strict quarantine rules may prevent the arrival of humanitarian supplies. For example, after the devastation caused by the tropical cyclone Harold in the Pacific Islands, the supplies sent by the Australian government could not be distributed immediately to avoid contagion.¹⁰ This situation is exacerbated by the potential lack of financial resources from the international community to support the affected nations, due to the need to cope with the economic impact caused by the outbreak.

Despite the limitations and assumptions in the results, data sets and models presented herein, they can still be relevant to inform decision makers in disaster risk mitigation and to raise risk awareness for the potential impact of earthquakes in the COVID-19 pandemic. The collection of more data (both in terms of quantity and quality) will be fundamental to carry out additional research to constrain some of the sources of uncertainty described in this study and ultimately improve the reliability and accuracy of the predictions.

Author's Note

Vitor Silva is currently affiliated with Faculty of Science and Technology, University Fernando Pessoa, Porto, Portugal.

Acknowledgments

The authors would like to thank Dr Marta Novak, Dr Josip Atalic, and Dr Mario Uros for the support in the interpretation of the data for Croatia; Dr Pierre Nouvellet for his support on the estimation of transmissibility and forecasting of new COVID-19 cases; and Dr Mauro Dolce for the valuable suggestions. The authors are also grateful for the support provided by the GEM Foundation.

Declaration of conflicting interests

The author(s) declared no potential conflicts of interest with respect to the research, authorship, and/or publication of this article.

Funding

The author(s) received no financial support for the research, authorship, and/or publication of this article.

Notes

1. Ministry of Health of Vanuatu, COVID-19 Updates: <https://covid19.gov.vu/>
2. Croatian Institute of Public Health: <https://www.koronavirus.hr/en>
3. <https://covid19.min-saude.pt/>
4. <https://github.com/dssg-pt/covid19pt-data>
5. <https://www.dssg.pt/>
6. <https://github.com/dssg-pt/covid19pt-data>
7. COVID-19 mortality rates: <https://ourworldindata.org/mortality-risk-covid>
8. <https://github.com/CSSEGISandData/COVID-19>
9. <https://www.worldometers.info/coronavirus/>
10. <https://reliefweb.int/report/vanuatu/cargo-restrictions-hamper-vanuatu-cyclone-recovery-0>

References

- Anderson R, May R (1991). *Infectious Diseases of Humans: Dynamics and Control*, Oxford, United Kingdom, Oxford University Press.
- AIR Worldwide (2013) Study of impact and the insurance and economic cost of a major earthquake in British Columbia and Ontario/Québec. *Report commissioned by the Insurance Bureau of Canada*. Available at: <http://assets.ibc.ca/Documents/Studies/IBC-EQ-Study-Full.pdf> (accessed 21 May 2020).
- Akkar S and Bommer J (2010) Empirical equations for the prediction of PGA, PGV and spectral accelerations in Europe, the Mediterranean region and the Middle East. *Seismological Research Letters* 81(2): 195–206.

- Amundsen EJ, Stigum H, Rottingen JA and Aalen O (2004) Definition and estimation of an actual reproduction number describing past infectious disease transmission: Application to HIV epidemics among homosexual men in Denmark, Norway and Sweden. *Epidemiology & Infection* 132(6): 1139–1149.
- Anhorn J and Khazai B (2014) Open space suitability analysis for emergency shelter after an earthquake. *Natural Hazards Earth System Sciences* 1(2): 4263–4297.
- Atkinson G and Boore D (2006) Earthquake ground-motion prediction equations for eastern North America. *Bulletin of the Seismological Society of America* 96(6): 2181–2205.
- Boire NA, Riedel VA, Parrish NM and Riedel S (2013) Lessons learned from historic plague epidemics: The relevance of an ancient disease in modern times. *Journal of Infectious Diseases and Preventive Medicine* 2(2): 1–17.
- Carvalho A, Zonno G, Franceschina G, Bilé Serra J and Campos Costa A (2008) Earthquake shaking scenarios for the Metropolitan Area of Lisbon. *Soil Dynamics and Earthquake Engineering* 28(5): 347–364.
- Cintron-Arias A, Castillo-Chavez C, Bettencourt LM, Lloyd AL and Banks HT (2009) The estimation of the effective reproductive number from disease outbreak data. *Mathematical Biosciences and Engineering* 6(2): 261–282.
- Coburn A and Spence R (2002) *Earthquake Protection*. 2nd ed. Chichester: John Wiley and Sons.
- Cori A, Ferguson NM, Fraser C and Cauchemez S (2013) A new framework and software to estimate time-varying reproduction numbers during epidemics. *American Journal of Epidemiology* 178(9): 1505–1512.
- Crowley H, Despotaki V, Rodrigues D, Silva V, Toma-Danila D, Riga E, Karatzetzu A, Zugic Z, Sousa L, Ozcebe S, Gamba P (2020). Exposure Model for European Seismic Risk Assessment. *Earthquake Spectra*. DOI: <https://doi.org/10.1177/8755293020919429>
- Detweiler ST and Wein AM (2017) The HayWired earthquake scenario: U.S. Geological Survey Scientific Investigations. Report 2017–5013. Available at: <https://doi.org/10.3133/sir20175013> (accessed 21 May 2020).
- Dolce M (2010) Emergency and post-emergency management of the Abruzzi Earthquake, theme-leader lecture. In: *14th European conference on earthquake engineering*, pubblicato (eds M Garevski and A Ansal), Ohrid, Macedonia, 3–8 September. Earthquake Engineering in Europe. Dordrecht: Springer.
- Dolce M and Di Bucci D (2015) Comparing recent Italian earthquakes. *Bulletin of Earthquake Engineering* 15: 497–533.
- DPC (2018) National risk assessment, Overview of the potential major disasters in Italy: Seismic, volcanic, tsunami, hydro-geological/hydraulic and extreme weather, droughts and forest fire risks. Technical report, Presidency of the Council of Ministers Italian Civil Protection Department, Rome, Italy, December.
- Emrich C and Cutter S (2011) Social vulnerability to climate-sensitive hazards in the southern United States. *Weather, Climate, and Society* 3(3): 193–208.
- Erdik M and Durukal E (2008) Earthquake risk and its mitigation in Istanbul. *Natural Hazards* 44(2): 181–197.
- FEMA P-58 (2012) *Seismic Performance Assessment of Buildings*. Washington, DC: FEMA.
- Ferguson NM, Laydon D, Nedjati-Gilani G, Imai N, Ainslie K, Baguelin M, Bhatia S, Boonyasiri A, Cucunubá Z, Cuomo-Dannenburg G, Dighe A, Dorigatti I, Fu H, Gaythorpe K, Green W, Hamlet A, Hinsley W, Okell LC, van Elsland S, Thompson H, Verity R, Volz E, Wang H, Wang Y, Walker PGT, Walters C, Winskill P, Whittaker C, Donnelly CA, Riley S and Ghani AC (2020) Impact of non-pharmaceutical interventions (NPIs) to reduce COVID-19 mortality and healthcare demand. *ImperialAcUk*:3–20. Available at: <https://www.imperial.ac.uk/media/imperial-college/medicine/mrc-gida/2020-03-16-COVID19-Report-9.pdf> (accessed 21 May 2020).
- Fraser C (2007) Estimating individual and household reproduction numbers in an emerging epidemic. *PLoS ONE* 2(1): e1758.
- Gatto M, Bertuzzo E, Mari L, Miccoli S, Carraro L, Casagrandi R and Rinaldo A (2020) Spread and dynamics of the COVID-19 epidemic in Italy: Effects of emergency containment measures.

- Proceedings of the National Academy of Sciences of the United States of America* 117(19): 10484–10491.
- Hale T, Angrist N, Kira B, Petherick A, Phillips T and Webster S (2020) Variation in government responses to COVID-19, version 5.0. *Blavatnik School of Government Working Paper*. Available at: www.bsg.ox.ac.uk/covidtracker (accessed 21 May 2020).
- Jalayer F, De Risi R and Manfredi G (2015) Bayesian Cloud Analysis: Efficient structural fragility assessment using linear regression. *Bulletin of Earthquake Engineering* 13(4): 1183–1203.
- Maier B and Brockmann D (2020) Effective containment explains subexponential growth in recent confirmed COVID-19 cases in China. *Science* 368(64492): 742–746.
- Martins L and Silva V (2020). Development of a fragility and vulnerability model for global seismic risk analyses. *Bulletin of Earthquake Engineering*. DOI: <https://doi.org/10.1007/s10518-020-00885-1>
- Mendes-Victor LA, Oliveira CS, Pais I and Teves-Costa P (1994) Earthquake damage scenarios in Lisbon for disaster preparedness. In: Tucker BE, Erdik M and Hwang CN (eds) *Issues in Urban Earthquake Risk. NATO ASI Series E, Applied Science*, Vol. 271. Dordrecht: Kluwer Academic Press, pp. 265–289.
- Nouvellet P, Cori A, Garske T, Blake IM, Dorigatti I, Hinsley W, Jombart T, Mills HL, Nedjati-Gilani G, Van Kerkhove MD, Fraser C, Donnelly CA, Ferguson NM and Riley S (2018) A simple approach to measure transmissibility and forecast incidence. *Epidemics* 22: 29–35.
- Oliveira C (2004) The influence of scale on microzonation and impact studies. In: Ansal A (ed.) *Recent Advances in Earthquake Geotechnical Engineering and Microzonation*, Chapter 2. Dordrecht: Kluwer Academic, pp. 27–65.
- Oliveira C (2008) Lisbon earthquake scenarios: A review on uncertainties, from earthquake source to vulnerability modelling. *Soil Dynamics and Earthquake Engineering* 28: 890–913.
- Pagani M, Garcia-Pelaez J, Gee R, Johnson K, Silva V, Simionato M, Styron R, Viganò D, Danciu L, Monelli D, Poggi V and Weatherill G (2020) The 2018 version of the Global Earthquake Model: Hazard component. *Earthquake Spectra*. DOI: 10.1177/8755293020931866
- Pagani M, Monelli D, Weatherill G, Danciu L, Crowley H, Silva V, Henshaw P, Butler L, Nastasi M, Panzeri L, Simionato M and Viganò D (2014) OpenQuake Engine: An open hazard (and risk) software for the Global Earthquake Model. *Seismological Research Letters* 85(3): 692–702.
- Pérez-Martín JJ, Romera Guirado FJ, Molina-Salas Y, Bernal PJ and Navarro JA (2017) Vaccination campaign at a temporary camp for victims of the earthquake in Lorca (Spain). *Human Vaccines & Immunotherapeutics* 13: 1714–1721.
- Petrazzi L, Striuli R, Polidoro L, Petrarca M, Scipioni R, Struglia M, Giorgini P, Necozone S, Festuccia V and Ferri C (2013) Causes of hospitalisation before and after the 2009 L'Aquila earthquake. *Internal Medicine Journal* 43: 1031–1034.
- Quigley M, Attanayake J, King A, Prideaux F (2020). A multi-hazards earth science perspective on the COVID-19 pandemic: the potential for concurrent and cascading crises. *Environment Systems and Decisions* 40: 199–215.
- Riley S, Fraser C, Donnelly CA, Ghani AC, Abu-Raddad LJ, Hedley AJ, Leung GM, Ho L-M, Lam T-H, Thach TQ, Chau P, Chan K-P, Lo S-V, Leung P-Y, Tsang T, Ho W, Lee K-H, Lau EMC, Ferguson NM and Anderson RM (2003) Transmission dynamics of the etiological agent of SARS in Hong Kong: Impact of public health interventions. *Science* 300(5627): 1961–1966.
- Sengezer B and Koç E (2005) A critical analysis of earthquakes and urban planning in Turkey. *Disasters* 29(2): 171–194.
- Silva V, Amo-Oduro D, Calderon A, Costa C, Dabbeek J, Despotaki V, Martins L, Pagani M, Rao A, Simionato M, Viganò D, Yepes-Estrada C, Acevedo A, Crowley H, Horspool N, Jaiswal K, Journeay M and Pittore M (2020) Development of a global seismic risk model. *Earthquake Spectra* 36(S1): 372–394.
- Silva V, Crowley H, Pagani M, Monelli D and Pinho R (2014a) Development of the OpenQuake engine, the Global Earthquake Model's open-source software for seismic risk assessment. *Natural Hazards* 72(3): 1409–1427.
- Silva V, Crowley H, Pinho R and Varum H (2014b) Seismic risk assessment for mainland Portugal. *Bulletin of Earthquake Engineering* 13(2): 429–457.

- Silva V, Marques M, Castro JM and Varum H (2015) Development and application of a real-time loss estimation framework for Portugal. *Bulletin of Earthquake Engineering* 13: 2493–2516.
- Sousa ML and Campos-Costa A (2009) Ground motion scenarios consistent with probabilistic seismic hazard disaggregation analysis. *Application to Mainland Portugal Bulletin of Earthquake Engineering* 7: 127–147.
- Spence R (ed.) (2007) *Earthquake Disaster Scenario Prediction and Loss Modelling for Urban Areas*. Pavia: IUSS Press.
- Suk J, Vaughan E, Cook R and Semenza J (2019) Natural disasters and infectious disease in Europe: A literature review to identify cascading risk pathways. *European Journal of Public Health*. Epub ahead of print 6 June. DOI: 10.1093/eurpub/ckz111.
- Tsiamis C, Poulakou-Rebelakou E and Marketos S (2013) Earthquakes and plague during Byzantine times: Can lessons from the past improve epidemic preparedness? *Acta Medico-Historica Adriatica* 11(1): 55–64.
- Vilanova S, Fonseca J, Oliveira C (2012). Ground-Motion for Seismic Hazard Assessment in Western Iberia. *Bulletin of the Seismological Society of America* 102:169–184.
- Watson J, Gayer M and Connolly M (2007) Epidemics after natural disasters. *Emerging Infectious Diseases* 13(1): 1–5.
- World Health Organization (WHO) (2005) Epidemic-prone disease surveillance and response after the tsunami in Aceh Province, Indonesia. *The Weekly Epidemiological Record* 80: 160–164.
- World Health Organization (WHO) (2006) Acute jaundice syndrome. Weekly Morbidity and Mortality Report. 23:8. (cited 2006 August 10). Available at: http://www.who.int/hac/crises/international/pakistan_earthquake/sitrep/Pakistan_WMMR_VOL23_03052006.pdf (accessed 21 May 2020).